

Slender planing surfaces

E. O. Tuck

Received: 6 February 2006 / Accepted: 5 December 2006 / Published online: 30 March 2007
© Springer Science+Business Media B.V. 2007

Abstract A theory for slender planing surfaces of general shape at high Froude number was formulated by Casling (J Eng Math (1978) 12:43–57). Although this theory was later extended by Casling and King (J Eng Math (1980) 14:191–205), it remains somewhat distant from application to actual planing vessel design. The present paper is an attempt to move the Casling theory a little in that direction. A modified formula connecting underwater hull shape and wetted planform is suggested here, which may be more suitable for numerical computation. Spraysheets and forces are also discussed, and a sprayless example hull is provided.

Keywords Planing · Slender · High Froude number · Wetted planform

1 Formulation

The task is to solve for flow of a stream at speed U around a fixed vessel whose hull geometry is defined by $y = Y(x, s)$ for some given function $Y(x, s)$, in a coordinate system with s directed from bow to stern, x to starboard, and y upward. We use a prime for derivatives with respect to s ; thus Y' is the longitudinal slope. We assume lateral symmetry, so $Y(-x, s) = Y(x, s)$.

It remains to specify *where* $Y(x, s)$ is given. In steady flow, the input hull geometry $Y(x, s)$ is relevant to the hydrodynamics only on a wetted planform $-b(s) < x < b(s)$. We shall assume the wetted planform to be pointed at the bow and never decreasing in width aft of the bow, i.e., $b(0) = 0$ and $b'(s) \geq 0$ for all $s > 0$. Outside of this wetted planform, $y = Y(x, s)$ defines the shape of the free surface, which is unknown in advance, and lies beneath the input (dry) hull.

However, in practice it is the whole (both wet and dry) input hull shape that is given, and an important intermediate objective is then to determine the half-beam function $b(s)$, i.e., to determine the actual extent of the wetted planform. It is this particular objective that is the focus of the present paper and of Casling [1] and Casling and King [2]. Once this task is carried out, further objectives such as determination of spraysheet properties and of hydrodynamic forces on the hull are then straightforward.

E. O. Tuck (✉)
Department of Applied Mathematics, The University of Adelaide, Adelaide 5005, Australia
e-mail: ernie.tuck@adelaide.edu.au

There are several assumptions made here and by Casling [1] to simplify this flow problem. Beside the usual classical hydrodynamical assumptions (irrotational steady flow of an incompressible inviscid fluid), these are:

- (1) infinite Froude number (high speed, or neglect of gravity),
- (2) small draft relative to both beam and length (flat ship),
- (3) small beam relative to length (slender planform), and
- (4) infinite water depth.

The combined effect of these assumptions is to reduce the flow problem to the task of solving in $y < 0$ the two-dimensional Laplace equation,

$$\phi_{xx} + \phi_{yy} = 0, \quad (1)$$

for the disturbance velocity potential $\phi(x, y, s)$, separately in each cross-section $s = \text{constant}$, subject to linearised boundary conditions on the plane $y = 0$, and $\phi \rightarrow 0$ as $y \rightarrow -\infty$. On the wetted body segment $|x| < b(s)$, $y = 0$, a linearised Neumann boundary condition,

$$\phi_y(x, 0, s) = UY'(x, s), \quad (2)$$

holds, with Y known. Outside of that segment, the linearised free-surface condition with zero gravity is just

$$\phi(x, 0, s) = 0, \quad |x| > b(s). \quad (3)$$

However, Eq. 2 still holds in $|x| > b(s)$, and then it relates the (unknown) free surface Y to the upward velocity component ϕ_y .

We also make use of the stream function $\psi(x, y, s)$, the harmonic conjugate of ϕ . Because ϕ and ψ are connected by the Cauchy–Riemann equations,

$$\phi_x = \psi_y, \quad \psi_x = -\phi_y, \quad (4)$$

the stream function ψ is known on the body segment $|x| < b(s)$ by x -integration of (2), namely

$$\psi(x, 0, s) = -U \int_0^x Y'(\xi, s) \, d\xi. \quad (5)$$

Again (5) also holds for $|x| > b(s)$, where it relates the (unknown) free-surface shape Y to the stream function ψ .

2 Flow solution

The above two-dimensional flow problem in the lower half-plane $y < 0$ is solved at each fixed s by use of the Plemelj relation [3, p. 42], [4, p. 170] between the harmonic conjugates ϕ and ψ , namely

$$\psi(x, 0, s) = -\mathcal{H}\phi(x, 0, s) \quad (6)$$

where \mathcal{H} is the Hilbert transform operator [4, p. 185], [5, p. 173], such that

$$\mathcal{H}f(x) = \frac{1}{\pi} \int_{-\infty}^{\infty} \frac{d\xi}{x - \xi} f(\xi) \quad (7)$$

for any function $f(x)$ defined for all real x , the integral being a Cauchy principal value.

In the present case, the free-surface condition (3) means that the infinite-range integral in (7) reduces to one over the finite range $(-b, b)$, for which we denote the finite Hilbert transform as \mathcal{H}_b . Now using a well-known inversion [4, p. 182], [5, p. 174] of the finite Hilbert transform, the appropriate (bounded and continuous) solution of (6) for ϕ on the body is

$$\phi(x, 0, s) = \sqrt{b^2(s) - x^2} \mathcal{H}_{b(s)} \frac{\psi(x, 0, s)}{\sqrt{b^2(s) - x^2}}. \tag{8}$$

This then provides the solution of the flow problem, since $\psi(x, 0, s)$ is known in $|x| < b(s)$ by (5).

We are also interested in values of the stream function ψ on the free surface outside of the body, e.g. for $x > b(s)$. Equation 6 still holds for such x , and implies when $\phi(x, 0, s)$ is given by (8) that

$$\psi(x, 0, s) = \sqrt{x^2 - b^2(s)} \mathcal{H}_{b(s)} \frac{\psi(x, 0, s)}{\sqrt{b^2(s) - x^2}}, \tag{9}$$

which can be x -differentiated to give the vertical velocity component via

$$\psi_x(x, 0, s) = -\frac{1}{\sqrt{x^2 - b^2(s)}} \mathcal{H}_{b(s)} \left[\psi_x(x, 0, s) \sqrt{b^2(s) - x^2} \right]. \tag{10}$$

Using (5) to relate ψ_x to Y' , this means that

$$Y'(x, s) = -\frac{1}{\sqrt{x^2 - b^2(s)}} \mathcal{H}_{b(s)} \left[Y'(x, s) \sqrt{b^2(s) - x^2} \right] \tag{11}$$

or on s -integration

$$Y(x, s) = -\int_0^s \frac{d\sigma}{\sqrt{x^2 - b^2(\sigma)}} \mathcal{H}_{b(\sigma)} \left[Y'(x, \sigma) \sqrt{b^2(\sigma) - x^2} \right], \tag{12}$$

which provides the free-surface shape in $x > b(s)$, given the hull shape in $|x| < b(s)$.

In fact, by continuity, Eq. 12 must also hold at the boundary $x = b(s)$ between planform and free surface. This then leads to the following key formula, connecting wetted perimeter and hull shape, namely

$$Y(b(s), s) = \int_0^s \frac{1}{\sqrt{b^2(s) - b^2(\sigma)}} Z(s, \sigma) d\sigma, \tag{13}$$

where

$$Z(s, \sigma) = -\frac{1}{\pi} \int_{-b(\sigma)}^{b(\sigma)} \frac{\sqrt{b^2(\sigma) - \xi^2}}{b(s) - \xi} Y'(\xi, \sigma) d\xi. \tag{14}$$

This is the same as Casling’s [1, Eq. 3.5] evaluated at $x = b(s)$. Note that the square root in the denominator of (13) is only defined when $b(s)$ is an increasing function of s , as assumed.

In the most general case, our task is to invert (13) subject to (14), to compute $b(s)$, given $Y(x, s)$.

3 Laterally constant longitudinal slope

Casling [1] discusses an important special case when $Z(s, \sigma)$ can be evaluated explicitly, namely that in which the slope $Y'(x, s) = Y'_0(s)$ is independent of x , or “laterally constant longitudinal slope”, LCLS for brevity. Without loss of generality we may assume that $Y_0(0) = 0$; thus LCLS hulls have

$$Y(x, s) = Y_0(s) + c(x) \tag{15}$$

for some $c(x)$. It is incorrect and misleading to conclude that $c(x) = Y(x, 0)$, since $Y(x, s)$ is only defined for $|x| < b(s)$, and hence for increasing $b(s)$ with $b(0) = 0$, $Y(x, s)$ is not defined for any $x > 0$ when $s = 0$.

Now for LCLS we have

$$Z(s, \sigma) = Y'_0(\sigma) \left[\sqrt{b^2(s) - b^2(\sigma)} - b(s) \right] \tag{16}$$

and hence (13) gives

$$Y(b(s), s) = Y_0(s) - b(s) \int_0^s \frac{Y'_0(\sigma)}{\sqrt{b^2(s) - b^2(\sigma)}} d\sigma \tag{17}$$

or

$$c(x) = -x \int_0^{s_0(x)} \frac{Y'_0(\sigma)}{\sqrt{x^2 - b^2(\sigma)}} d\sigma, \tag{18}$$

which is Casling’s Eq. 4.1; see [1]. Equation 18 can be inverted explicitly as an Abel integral equation [5, p. 39], to yield

$$Y_0(s_0(x)) = -\frac{2}{\pi} \int_0^x \frac{c(\xi)}{\sqrt{x^2 - \xi^2}} d\xi \tag{19}$$

or

$$Y_0(s) = -\frac{2}{\pi} \int_0^{b(s)} \frac{c(\xi)}{\sqrt{b(s)^2 - \xi^2}} d\xi \tag{20}$$

$$= -\frac{2}{\pi} \int_0^{\pi/2} c(b(s) \sin \theta) d\theta, \tag{21}$$

from which $s_0(x)$ or $b(s)$ can be found, given both $Y_0(s)$ and $c(x)$.

A variety of example LCLS hulls are discussed in [1] and [2]. In particular, V-shaped sections $c(x) = \gamma|x|$ with constant deadrise angle γ have $Y_0(s) = -(2/\pi)\gamma b(s)$, so $Y(x, s) = \gamma(|x| - (2/\pi)b(s))$. Hence the wetted waterline $x = b(s)$ is of the same general shape as the keel line $y = -(2/\pi)\gamma b(s)$, with the height $Y(b(s), s)$ of the contact point or spray root a fixed multiple $\pi/2 - 1 \approx 0.57$ of the local draft. In the further specialisation to

$$Y(x, s) = -\alpha s + \gamma|x| \tag{22}$$

with constant angle of attack α , this confirms the generally accepted result [6] that V-shaped cross-sections yield triangular wetted planforms $b(s) = \beta s$, with $\beta = (\pi/2)\alpha/\gamma$.

Other flow quantities of interest for LCLS hulls are

$$\psi(x, 0, s) = -UY'_0(s)x \tag{23}$$

and

$$\phi(x, 0, s) = UY'_0(s)\sqrt{b^2 - x^2}. \tag{24}$$

It is also worth noting some sign properties that follow from (21). Thus $c(x) > 0$ implies $Y_0(s) < 0$. Also, on s -differentiation of (21), $c'(x) > 0$ implies (so long as $b'(s) > 0$) that $Y'_0(s) < 0$. That is, positive deadrise combined with increasing waterline width guarantees increasing keel depth. Conversely, positive deadrise combined with increasing keel depth guarantees increasing waterline width. Although these are explicit properties of LCLS hulls, it is possible that they also hold for more general families of slender planing surfaces.

4 Numerical solution

In the general case, we must resort to (iterative) numerical solution for $b(s)$ of the original equation (13) subject to (14). The special case of LCLS is, however, instructive in suggesting to first add and subtract a term from the numerator of (14). Thus we may write

$$Z(s, \sigma) = Z_0(s, \sigma) + Z_1(s, \sigma), \tag{25}$$

where (analogous to (16))

$$Z_0(s, \sigma) = Y'(b(\sigma), \sigma) \left[\sqrt{b^2(s) - b^2(\sigma)} - b(s) \right] \tag{26}$$

and

$$Z_1(s, \sigma) = -\frac{1}{\pi} \int_{-b(\sigma)}^{b(\sigma)} \frac{\sqrt{b^2(\sigma) - \xi^2}}{b(s) - \xi} [Y'(\xi, \sigma) - Y'(b(\sigma), \sigma)] d\xi. \tag{27}$$

In numerical implementations, we make use of lateral symmetry to reduce the integral in (27) to the range $(0, b(\sigma))$.

Because the integrand of (27) vanishes like the 3/2 power of distance from the ends of the range of ξ -integration, we may expect reasonable accuracy from conventional numerical quadratures on a uniform grid, better than would be achieved from (14) without the subtraction. Also, this property indicates that, when $\sigma \rightarrow s$,

$$Z_1 = A + B(s - \sigma) + C(s - \sigma)^{3/2} + O(s - \sigma)^2 \tag{28}$$

for some constants A, B, C . On the other hand, as is clear from the explicit form (26) of Z_0 , the full Z -function also contains a term in $(s - \sigma)^{1/2}$.

Now (13) states that

$$Y(b(s), s) = \int_0^s Y'(b(\sigma), \sigma) d\sigma + \int_0^s \frac{Z_1(s, \sigma) - b(s)Y'(b(\sigma), \sigma)}{\sqrt{b^2(s) - b^2(\sigma)}} d\sigma. \tag{29}$$

Note that for LCLS hulls, $Y'(\xi, \sigma) = Y'(b(\sigma), \sigma) = Y'_0(\sigma)$ and hence $Z_1 \equiv 0$, so (29) reduces to (17).

Equation 29 is equivalent to [2, Eq. 4.1], which was used by them as a basis for computation of wetted perimeters $b(s)$. However, that equation was written in terms of a function $c(x)$ which is strictly only defined for LCLS as in (15). Casling and King [2] also subtracted $Y'(b(s), \sigma)$ rather than $Y'(b(\sigma), \sigma)$, and the former is not defined when $\sigma < s$.

We use (29) for computation purposes on fixed s - and x -grids, but with a careful treatment of the inverse-square-root end singularity (28) in the second term at $\sigma = s$. Casling and King [2] used a “re-scaled” σ -grid, re-computed with data interpolation at each new s , with square-root biased points near $\sigma = s$; however, this re-gridding and interpolation is not necessary with the present formula (29).

Essentially the present numerical method advances in the s -direction from bow to stern, assuming when computing at a particular station s that $b(\sigma)$ is already known at all earlier stations $\sigma < s$. Then our task is to determine the single unknown value $b(s)$ at the current station s .

Given a trial value for $b(s)$, the ξ -integral (27) for $Z_1(s, \sigma)$ is evaluated for each $\sigma < s$, by a trapezoidal-like quadrature that is exact when the slope $Y'(\sigma, \xi)$ is linear in ξ . Nearly all of this integral on $(0, b(\sigma))$ can be done with a fixed uniformly spaced x -grid, but since in general the endpoint $\xi = b(\sigma)$ does not coincide with a gridpoint, we also need to add a small extra contribution to Z_1 from the segment between $\xi = b(\sigma)$ and the x -grid point immediately below it.

Having thus computed $Z = Z_0 + Z_1$, we then compute the σ -integral on the right of (13), for which (on a uniformly spaced s -grid) we need a special set of weights taking into account the inverse-square-root singularity in the integrand at $\sigma = s$. Finally, we use the secant rule [7, p. 933] to iterate on the unknown value of $b(s)$ until this last integral is equal to $Y(b(s), s)$ as required.

The accuracy of this numerical method depends in general on the number N_s of stations in the vessel's length, and the number N_x of buttocks in its maximum half-beam. However, the special quadratures described above are such that exact results are generated for the constant-deadrise V-shaped hull (22), and also near-exact results (since Z is computed exactly) for any hull with V-shaped sections, even when the deadrise angles are not constant.

A more severe numerical test is the U-shaped LCLS hull,

$$Y(x, s) = -\alpha s^2 + \gamma x^2, \quad (30)$$

with constant α and β , for which the exact solution (20) again indicates a triangular wetted planform $b(s) = \beta s$, but now with $\beta = \sqrt{2\alpha/\gamma}$. We find for this case convergence rates of N_s^{-2} and $N_x^{-3/2}$, thus enabling about three figures of accuracy with $N_s = N_x = 50$. A minor but annoying difficulty is establishing the solution at the first station near the bow, when the secant rule is hard to start. At subsequent stations, extrapolation yields a good starting guess for $b(s)$.

The present computer program appears to work well for arbitrary smooth hulls $Y(x, s)$. Further work is needed, however, for hulls with sharp edges or chines, special cases of which are treated in [2], and also to improve starting (near bow) performance of the iteration process.

5 Leading-edge singularity and spray

Letting $x \rightarrow b(s)_+$ in (10), we find that

$$\psi_x(x, 0, s) \rightarrow -\frac{F(s)}{\sqrt{x^2 - b^2}}, \quad (31)$$

where

$$F(s) = \mathcal{H}_{b(s)} \left[\psi_x(x, 0, s) \sqrt{b^2(s) - x^2} \right] \tag{32}$$

evaluated at $x = b(s)$. That is, making use of the fact that $\psi_x = -UY'$ is an even function of x ,

$$F(s) = -U \frac{b(s)}{\pi} \int_{-b(s)}^{b(s)} \frac{Y'(x, 0, s)}{\sqrt{b^2(s) - x^2}} dx. \tag{33}$$

Equation 31 shows that (so long as $F(s)$ is non-zero) the vertical velocity component $v = -\psi_x$ at the free surface becomes infinite like an inverse square root at the point where the free surface meets the body, and hence the free surface is locally vertical. Such a local singularity and vertical slope models in this linearised theory the thin but nonlinear local spray sheet at the body–water junction. The coefficient $F(s)$ of this singularity is now known by (33), given the body longitudinal slope function Y' , and its magnitude varies with station s .

For LCLS, the spray-sheet strength is

$$F(s) = -Ub(s)Y'_0(s) \tag{34}$$

and in the special case $c(x) = \gamma|x|$ of V-shaped sections, this becomes

$$F(s) = \frac{2}{\pi} U\gamma b(s)b'(s), \tag{35}$$

which is positive for increasing $b(s)$.

We expect that $F(s) \geq 0$ in general; in particular, it is likely that $F(s) < 0$ would imply decreasing $b(s)$, which we have ruled out. Further work is needed to clarify this and other issues associated with wetted planforms that decrease in width. However, zero spray-sheet strength is not ruled out, and we show later an example with $F(s) = 0$ for all s .

6 Hull pressure and forces

The hydrodynamic pressure $p = P(x, s)$ on the body (excess over atmospheric) is related to ϕ by the linearised Bernoulli equation

$$P(x, s) = -\rho U \phi_s(x, 0, s), \tag{36}$$

where ρ is the constant water density. The net lift $L(s)$ on the hull from the bow $s = 0$ to a general station s is the double integral over the planform of this pressure, and it is convenient to write this as the lateral integral

$$L(s) = \int_{-b(s)}^{b(s)} Q(x, s) dx \tag{37}$$

of a stripwise loading along the buttock at fixed x , namely

$$Q(x, s) = \int_{s_0(x)}^s P(x, \sigma) d\sigma. \tag{38}$$

Now it follows from (36) that Q is proportional to ϕ on the body, specifically

$$Q(x, s) = -\rho U \phi(x, 0, s) \quad (39)$$

and hence Q is now also known by (8). For example a LCLS hull has

$$Q(x, s) = -\rho U^2 Y'_0(s) \sqrt{b^2(s) - x^2} \quad (40)$$

so it has lift

$$L(s) = -\frac{\pi}{2} \rho U^2 Y'_0(s) b(s)^2. \quad (41)$$

The drag is at least formally given by

$$D(s) = - \int_{-b(s)}^{b(s)} dx \int_{s_0(x)}^s d\sigma Y'(x, \sigma) P(x, \sigma). \quad (42)$$

However, there are a number of still-unresolved issues relating to drag of slender planing hulls, including the role of leading edge suction or spray drag, and of pressure drag at the stern. This is left for further work.

Also for further work is the true dynamic problem for freely planing vessels. That is, in the present paper we have assumed that the vessel is fixed with geometry specified by $y = Y(x, s)$, as if held rigidly in a frame while a stream U passes by. The real planing problem allows the vessel to trim in response to hydrodynamic and propulsive forces, and the wetted planform is then profoundly influenced by this trim. However, the present work is still relevant, providing we assume that the equilibrium trimmed orientation is known.

7 A sprayless example

Suppose that the body has a longitudinal slope that varies quadratically with respect to x at every station s , from a (bow-up) value $-\alpha$ at $x = 0$ to a bow-down value $+\alpha$ at $x = b(s)$. The local centreline angle of attack $\alpha = \alpha(s)$ in general could vary with station s . That is,

$$Y'(x, s) = -\alpha(s) + 2\alpha(s) \frac{x^2}{b(s)^2}. \quad (43)$$

Then we find from (5) that in $|x| < b(s)$,

$$\psi(x, 0_-, s) = U\alpha x \left(1 - \frac{2}{3} \frac{x^2}{b^2}\right) \quad (44)$$

and from (8) that

$$\phi(x, 0, s) = -\frac{2}{3} U\alpha b \left[1 - \frac{x^2}{b^2}\right]^{3/2}. \quad (45)$$

Because this potential ϕ vanishes together with its x -derivative at the edge $x = b$, there is no spray, and this is confirmed by checking from (33) that the spraysheet strength $F(s)$ is zero for all s .

Now for $x \geq b(s)$, the free-surface slope is given by (11) as

$$Y'(x, s) = -\alpha + 2\alpha \left[\frac{x^2}{b^2} - \frac{x}{b} \sqrt{\frac{x^2}{b^2} - 1} \right], \tag{46}$$

which we can check agrees with (43) at $x = b$, and tends to zero as $x \rightarrow +\infty$. Also the loading is

$$Q(x, s) = \frac{2}{3} \rho U^2 \alpha b \left[1 - \frac{x^2}{b^2} \right]^{3/2}, \tag{47}$$

so the lift is

$$L(s) = \frac{\pi}{4} \rho U^2 \alpha b^2, \tag{48}$$

which is exactly half of that given by (41) for a LCLS hull with the same keel slope $Y'_0(s) = -\alpha(s)$.

The above holds for any s variation of $\alpha(s)$ and $b(s)$. To find the actual body shape $Y(x, s)$ we must integrate (43) and (46) with respect to s , which requires some assumption about the form of $\alpha(s)$ and $b(s)$. For example, suppose the hull has a straight keel ($\alpha = \text{constant}$), and a triangular wetted planform $b(s) = \beta s$ for some constant β .

Then we find a free-surface elevation

$$Y(x, s) = -\alpha s - 2\alpha \frac{x}{\beta} (\tan \theta - 2\theta) \tag{49}$$

in $x \geq b$, where

$$\sin 2\theta = \frac{\beta s}{x}, \tag{50}$$

and a parabolic body section

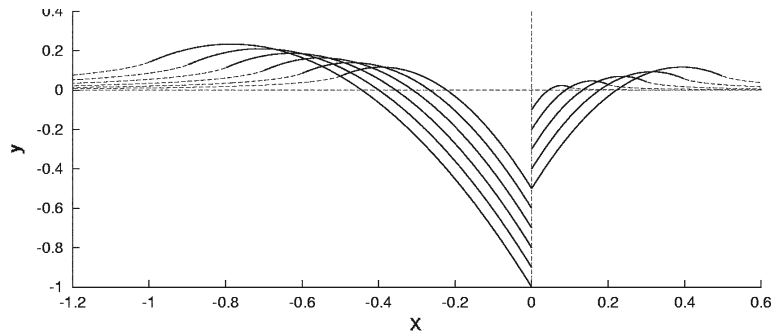
$$Y(x, s) = -\alpha s + \left(\frac{\pi \alpha}{\beta} \right) |x| - \left(\frac{2\alpha}{s\beta^2} \right) x^2 \tag{51}$$

in $|x| \leq b$, which agree at the body–water junction $x = b = \beta s$, where $\theta = \pi/4$.

The keel line of this body at $x = 0$ is $Y = -\alpha s$, at positive angle of attack α , so becoming deeper linearly as we move along the body. On the other hand, the body–water junction $x = b$ is at a positive and increasing height $Y = (\pi - 3)\alpha s$, above the undisturbed water level by a multiple ≈ 0.14 of the local keel depth. The maximum height of the section at s is $Y = (\pi^2/8 - 1)\alpha s$, above the undisturbed water level by a multiple ≈ 0.23 of the local keel depth, and this peak occurs at $x/b = \pi/4 \approx 0.79$. The section is at the undisturbed water level $Y = 0$ when $x/b = (\pi - \sqrt{\pi^2 - 8})/4 \approx 0.44$. The section is locally V-shaped at its keel, with constant positive deadrise angle $\pi\alpha/\beta$, but slopes downward at the body–water junction, at a negative angle $(\pi - 4)\alpha/\beta$ to the horizontal. Because there is no spray, the free surface leaves the body smoothly at this point with continuous downward lateral slope; this is in contrast to bodies generating a spray sheet, where the free-surface slope at the junction is infinite in this linearised theory.

Figure 1 shows sections of this hull (heavy lines) together with free-surface continuations (light lines).

Fig. 1 Offsets for a hull that generates no spray



8 Conclusions

The slender high-speed planing-surface theory of Casling [1] is suitable for study and design of planing surfaces of quite general smooth shape. However, in its original highly mathematical form it is difficult to use, and there are also some numerical problems in its implementation. The present paper is an attempt to remedy some of these difficulties. The extension in [2] to sharp-edged surfaces also needs some re-interpretation, which is left for further work.

Appendix: Laterally linear longitudinal slope

A somewhat more general class of hulls allows $Z(s, \sigma)$ to be evaluated exactly, namely

$$Y(x, s) = Y_0(s) + c(x) + \gamma(s)|x| \tag{52}$$

for general functions $Y_0(s)$, $c(x)$ and $\gamma(s)$. Since

$$Y'(x, s) = Y'_0(s) + \gamma'(s)|x|, \tag{53}$$

the longitudinal slope is a general linear function of x , so this class may be called “laterally linear longitudinal slope”, or LLLS. Alternatively, this hull has a general longitudinal variation in its deadrise angle $Y_x(0_+, s) = c'(0_+) + \gamma(s)$ at the keel.

Now we find for LLLS

$$Z(s, \sigma) = -Y'_0(\sigma)b(s) [1 - \cos \theta] - \frac{2}{\pi} \gamma'(\sigma)b(s)^2 [\sin \theta - \theta \cos \theta], \tag{54}$$

where $\sin \theta = b(\sigma)/b(s)$. The first term of (54) agrees with (16) for LCLS hulls where $\gamma'(\sigma) = 0$.

Now the equivalent for LLLS of (18) is (with $\sin \theta = b(\sigma)/x$)

$$c(x) + \gamma(s_0(x))x = -x \int_0^{\pi/2} \frac{Y'_0(\sigma)}{b'(\sigma)} d\theta - \frac{2}{\pi} x^2 \int_0^{\pi/2} \frac{\gamma'(\sigma)}{b'(\sigma)} [\sin \theta - \theta \cos \theta] d\theta. \tag{55}$$

If $b(s)$, $\gamma(s)$ and $c(x)$ are all given, the solution (21) for $Y_0(s)$ can still be used but with a modified $c(x)$, i.e.,

$$Y_0(s) = -\frac{2}{\pi} \int_0^{\pi/2} \bar{c}(b(s) \sin \theta) d\theta, \tag{56}$$

where

$$\bar{c}(x) = c(x) + \gamma(s_0(x))x + \frac{2}{\pi}x^2 \int_0^{\pi/2} \frac{\gamma'(\sigma)}{b'(\sigma)} [\sin \theta - \theta \cos \theta] d\theta. \tag{57}$$

The particular case of a triangular waterplane with $b(s) = \beta_1 s$, and a linearly varying deadrise angle with $\gamma(s) = \gamma_1 s$, gives

$$\bar{c}(x) = c(x) + \left(\frac{4\gamma_1}{\pi\beta_1}\right)x^2, \tag{58}$$

so

$$Y_0(s) = Y_1(s) - \left(\frac{2}{\pi}\gamma_1\beta_1\right)s^2, \tag{59}$$

where $Y_1(s)$ is as given by (21) for LCLS hulls. This is so for any fixed section shape $c(x)$, or equivalently determines the section shape for any given keel profile $y = Y_0(s)$.

In the further specialisation to V-shaped sections $c(x) = \gamma_0|x|$, we have finally

$$Y(x, s) = (\gamma_0 + \gamma_1 s) \left(|x| - \frac{2}{\pi}\beta_1 s \right). \tag{60}$$

The keel draft $-Y(0, s) = (2\beta_1/\pi)(\gamma_0 s + \gamma_1 s^2)$ then varies quadratically along the hull. The case $\gamma_1 < 0$ with decreasing deadrise angle $Y_x(0+, s) = \gamma_0 - |\gamma_1|s$ models some current designs. In that case the keel reaches its lowest point at station $s = \gamma_0/(2|\gamma_1|)$ when the deadrise angle has halved relative to its value γ_0 at the bow. Then (so long as the waterplane continues to increase in width linearly) the keel rises again until at station $s = \gamma_0/|\gamma_1|$ it reaches the undisturbed water level, with the section then flat and horizontal. Any further continuation aft maintaining a triangular waterplane would require inverted-V tunnelled sections.

References

1. Casling EM (1978) Planing of a low-aspect-ratio flat ship at infinite Froude number. J Engng Math 12:43–57
2. Casling EM, King G (1980) Calculation of the wetted area of a planing hull with a chine. J Engng Math 14:191–205
3. Muskhelishvili NI (1953) Singular integral equations, Moscow 1946, English translation by Radok JRM. Nordhoff, Groningen
4. Newman JN (1977) Marine hydrodynamics. MIT Press, Cambridge, Massachusetts
5. Tricomi FG (1957) Integral equations. Interscience, New York
6. Savitsky D (1964) Hydrodynamic design of planing hulls. J Marine Technology 1:71–95
7. Kreyszig E (1993) Advanced engineering mathematics, 7th edn. Wiley, New York